The steel fibers (Beka-Shield) were made of No. 304 austenitic stainless steel, as obtained from Bekaert Fiber Technologies (Marietta, GA). The fiber diameter was 8 μm. The fiber length was 6 mm. The fibers included 10 wt.% (47 vol.%) of a polyvinyl alcohol (PVA) binder, which was hydrophylic and dissolved in water during cement mixing, thus allowing fiber dispersion.

The carbon fibers were isotropic pitch based, unsized, and of length ~ 5 mm, diameter 15 μm and density 1.6 g/cm^3, as obtained from Ashland Petroleum Co. (Ashland, Kentucky). The fiber resistivity was 3.0 x 10^{-3} Ω.cm. Ozone treatment of the fibers [4] was performed to improve the fiber-matrix bond.

Silica fume was used as an admixture when carbon fibers were used. Silica fume (Elkem Materials, Inc., Pittsburgh, PA, EMS 965) was used in the amount of 15% by mass of cement. The methylcellulose, used along with silica fume in the amount of 0.4% by mass of cement, was Dow Chemical Corp., Midland, MI, Methocel A15-LV. The defoamer (Colloids, Inc., Marietta, GA, 1010) used along with methylcellulose was in the amount of 0.13 vol.%.

Three types of cement paste were prepared, namely (i) plain cement paste, which consists of cement and water, (ii) steel-fiber cement paste, which consists of cement, water, steel fibers in the amount of 0.90% by mass of cement, corresponding to 0.18 vol.%, and PVA in the amount of 0.1% by mass of cement, corresponding to 0.16 vol.%, and (iii) carbon-fiber silica-fume cement paste, which consists of cement, water, silica fume, methylcellulose, and carbon fibers in the amount of 1.0% by mass of cement, corresponding to 1.0 vol.%.

A rotary mixer with a flat beater was used for mixing. Methylcellulose (if applicable) was dissolved in water and then the defoamer (if applicable) was added and stirred by hand for about 2 min. Then the methylcellulose mixture (if applicable), cement, water, silica fume (if applicable) and fibers were mixed in the mixer for 5 min. After pouring into oiled molds, an external electrical vibrator was used to facilitate compaction and decrease the amount of air bubbles. The samples were demolded after 1 day and cured in air at room temperature (relative humidity = 100%) for 28 days.

Specimens were in the form of cylindrical discs of diameter (12.3 mm) and thickness 2.0 mm. A specimen, after mechanical polishing on both sides by using alumina particles of size 0.25 μm, was sandwiched by two copper discs (similarly polished) of diameter 12.3 mm at a pressure of 1.68 kPa, unless noted otherwise. The copper discs served as electrical contacts. Silver paint was applied between the specimen and each copper disc in case of piezoelectric testing. Due to the small thickness, preferred orientation of the fibers in the plane of the specimen disc was bound to occur.

The impedance was measured along the thickness of the specimen using the two-probe method and an RLC meter (QuadTech 7600) at frequencies ranging from 10 kHz to 1 MHz. The magnitude of voltage applied across the thickness (2 mm) of a specimen was 1.000 V. Hence, the magnitude of the applied electric field was 500 V/m. The resistance and reactance were obtained from the impedance by assuming that they were in series connection. The capacitance was obtained from the reactance. The dielectric constant was obtained from the capacitance. Six specimens of each type were tested.

To show that the dielectric constant measurement using the method described above was accurate, measurement was made on a Kapton (a polyimide by DuPont) film. The known dielectric constant of Kapton is 3.9 at 1 kHz. Measurement in this work at 1 kHz gave a value of 3.9 also.

For testing the piezoelectric behavior, during the impedance measurement, compressive stress was applied to the sandwich, so that the stress was parallel to the direction of impedance measurement. The stress (repeated loading at increasing stress amplitudes within the elastic regime) was provided by a hydraulic mechanical testing system (MTS Model 810). The minimum compressive stress was 1.68 kPa. Six specimens of each type were tested.

The longitudinal piezoelectric coupling coefficient d was obtained from the equation

$$d = \varepsilon_o E \left| \frac{\partial \kappa}{\partial \sigma} \right| \qquad (1)$$

where κ is the relative dielectric constant, σ is the stress, E is the electric field amplitude (500 V/m) and ε_o is the permittivity of free space. Thus, d is proportional to the change in κ per unit change in stress.

The piezoelectric voltage coefficient g was obtained from the equation

$$g = \frac{d}{(\kappa - 1)\varepsilon_o} \qquad (2)$$

The voltage change ∂V resulting from a stress change $\partial\sigma$ was calculated by using the equation

$$\partial V = \ell g \partial \sigma, \qquad (3)$$

where ℓ is the length of the specimen in the direction of polarization. The value of ∂V can be enhanced by increasing g, which can be increased by increasing d or decreasing κ, as shown by Eq. (2).

For testing the pyroelectric behavior, the measurement of κ was conducted above, at and below room temperature. Temperatures below room temperature (down to –4°C) were attained by putting the specimen in a freezer with temperature control. Temperatures above room temperature (up to 35°C) were attained by using a furnace that provided resistance heating.

The pyroelectric coefficient p is given by

$$p = \frac{\partial P}{\partial T} = \varepsilon_o E \frac{\partial \kappa}{\partial T}, \quad (4)$$

where P is the polarization, T is the temperature, ε_o is the permittivity of free space (8.85×10^{-12} C/V.m) and E is the electric field (500 V/m).

The voltage change ∂V resulting from a temperature change ∂T in a pyroelectric material can be calculated by using the equations

$$\partial E = \frac{\partial P}{\varepsilon_o (\kappa - 1)} \quad (5)$$

$$\partial V = \ell \partial E \quad (6)$$

and

$$\partial P = p \partial T, \quad (7)$$

where ∂E is the change in electric field. The value of ∂V can be enhanced by increasing p or decreasing κ, as shown by Eq. (7) and (5) respectively.

FIBER REINFORCED CEMENT FOR PIEZOELECTRICITY

The direct piezoelectric effect was observed in cement pastes by voltage measurement (33) and by observing the effect of stress on the electric polarization (34). It is attributed mainly to the movement of ions in response to stress.

The direct piezoelectric effect attained by using steel fibers (8 μm diameter) corresponds to a longitudinal piezoelectric coupling coefficient $d = 3 \times 10^{-11}$ m/V and piezoelectric voltage coefficient $g = 1 \times 10^{-3}$ m^2/C. These values are comparable to those of the conventional ceramic piezoelectric material lead zirconotitanate, i.e., $PbZrO_3$-$PbTiO_3$ solid solution, or, in short, PZT, as similarly measured. The similarity in d and g occurs in spite of the differences in mechanism and in material texture. In the cement case, the mechanism relates to the movement of the mobile ions under stress. In the case of conventional ceramic piezoelectric materials, the mechanism relates to the small change in spacing between ions of opposite charge under stress.

Table 1 shows the comparative piezoelectric performance of various cement pastes and PZT. The stainless steel fiber (8 μm diameter, 1.0% by mass of cement) cement paste gives the highest values of d and κ, while PZT gives the highest g. The carbon fiber (15 μm diameter, 1.0% by mass of cement) cement paste has much lower d than the steel fiber cement paste, but, due to its much lower κ, it gives g that is similar to that of the steel fiber cement paste. The overall performance in terms of both d and g is comparable between steel fiber cement paste and PZT.

The change in voltage obtained in the direct piezoelectric effect stems from the change in electric field. For the same electric field change, the voltage change is larger when the specimen length in the field direction is larger, as shown by Eq. (3). Due to the low cost and structural usage of cement, practical dimensions tend to be larger for cement than PZT. As a consequence, the voltage change obtained by using cement can be large compared to the typical voltage changes obtained by using PZT.

Fig. 1-3 show the relative dielectric constant (κ) and the applied stress (negative for compression) during repeated compressive loading of plain cement paste (without admixture), carbon fiber cement paste and steel fiber cement paste respectively. For all three pastes, κ increases (i.e., the reactance decreases) upon loading and the piezoelectric effect is partially reversible. The greater the stress amplitude, the more κ increases. The longitudinal piezoelectric coupling coefficient d, as averaged over the first half of the first stress cycle for each specimen, is shown in Table 1 for each of the pastes.

For all three pastes, the piezoelectric coupling coefficient d varies with stress. In general, the magnitude of d tends to decrease nonlinearly with increasing stress magnitude, such that the decrease occurs mainly at stress magnitudes below 1 MPa. The decrease in the magnitude of d with increasing stress magnitude is essentially reversible.

FIBER REINFORCED CEMENT FOR PYROELECTRICITY

Fig. 4-6 give the variation of κ with temperature for three frequencies (10 kHz, 100 kHz and 1 MHz) for plain cement paste, carbon fiber cement paste and steel fiber cement paste respectively. For each paste, at any temperature, κ decreases with increasing frequency, as expected; at any frequency, the lower the temperature, the lower is κ. The κ value at any combination of frequency and temperature is much higher for the steel fiber cement paste than carbon fiber cement paste or plain cement paste, probably due to the ions provided by PVA in the former and the functional groups on the steel fiber surface in the former.

Table 2 gives the values of pyroelectric coefficient p for different frequencies. The pyroelectric coefficient decreases with increasing frequency, as expected. The change in polarization is believed to involve ion movement, which is affected by the temperature and the frequency. The coefficient p increases in the order: plain cement paste, carbon fiber cement paste, and steel fiber cement paste.

The pyroelectric coefficient of steel fiber cement paste is below those of barium titanate and polyvinylidene fluoride by three orders of magnitude. Nevertheless, for $\kappa = 2500$ (the value for steel fiber cement paste at room temperature and 10 kHz) and for $p = 6.1 \times 10^{-8}$ C/m^2.K (the value for steel fiber cement paste at room temperature), a change in temperature of 10^{-3} K gives a change in electric field of 3×10^{-3} V/m. For a cement paste of thickness 1 cm, this change in electric field results in a voltage change of 30 μV (a measurable

quantity). A similar calculation for the case of carbon fiber cement paste gives a voltage change of 70 μV. A similar calculation for the case of plain cement paste also gives a voltage change of 70 μV. The voltage is higher for plain cement paste and carbon fiber cement paste than steel fiber cement paste in spite of the lower values of p for plain cement paste and carbon fiber cement paste, because κ is much higher for steel fiber cement paste than plain cement paste or carbon fiber cement paste. The voltage is the same for plain cement paste and carbon fiber cement paste in spite of the lower value of p for plain cement paste, because κ is higher for carbon fiber cement paste than plain cement paste.

CONCLUSION

Cement paste containing short steel fibers (8 μm diameter) and PVA exhibits attractive piezoelectric and pyroelectric behavior. The piezoelectric coupling coefficient and voltage coefficient are comparable to those of PZT, although the pyroelectric coefficient is low. Plain cement paste and carbon fiber cement paste have much lower values of the piezoelectric coupling coefficient and pyroelectric coefficient compared to steel fiber cement paste, but their much lower values of the relative dielectric constant result in piezoelectric voltage coefficient and pyroelectric voltage that are comparable to or even higher than those of steel fiber cement paste. The pyroelectric coefficient is higher for carbon fiber cement paste than plain cement paste, but carbon fiber cement paste and plain cement paste are comparable in the piezoelectric coupling coefficient, piezoelectric voltage coefficient and pyroelectric voltage.

ACKNOWLEDGEMENT

This work was supported by the National Science Foundation, U.S.A.

REFERENCES

1. Chung, D.D.L., *Self-Monitoring Structural Materials,* Mater. Sci. Eng. Rev., R22(2), 1998, pp. 57-78.

2. Wang, X., Fu, X. and Chung, D.D.L., *Strain Sensing Using Carbon Fiber,* J. Mater. Res., 14(3), 1999, pp. 790-802.

3. Wen, S., Wang, S. and Chung, D.D.L., *Piezoresistivity in Continuous Carbon Fiber Polymer-Matrix and Cement-Matrix Composites,* J. Mater. Sci., 35(14), 2000, pp. 3669-3675.

4. Fu, X., Lu, W. and Chung, D.D.L., *Ozone Treatment of Carbon Fiber for Reinforcing Cement,* Carbon, 36(9), 1998, pp. 1337-1345.

5. Fu, X. and Chung, D.D.L., *Effect of Curing Age on the Self-Monitoring Behavior of Carbon Fiber Reinforced Mortar,* Cem. Concr. Res., 27(9), 1997, pp. 1313-1318.

6. Fu, X., Ma, E., Chung, D.D.L. and Anderson, W.A., *Self-Monitoring in Carbon Fiber Reinforced Mortar by Reactance Measurement,* Cem. Concr. Res., 27(6), 1997, pp. 845-852.

7. Chen, P.-W. and Chung, D.D.L., *Carbon Fiber Reinforced Concrete as an Intrinsically Smart Concrete for Damage Assessment During Static and Dynamic Loading,* ACI Mater. J., 93(4), 1996, pp. 341-350.

8. Chen, P.-W. and Chung, D.D.L., *Concrete as a New Strain/Stress Sensor,* Composites, Part B, 27B, 1996, pp. 11-23.

9. Chen, P.-W. and Chung, D.D.L., *Carbon Fiber Reinforced Concrete as a Smart Material Capable of Non-Destructive Flaw Detection,* Smart Mater. Struct., 2, 1993, pp. 22-30.

10. Mao, Q., Zhao, B., Sheng, D. and Li, Z., *Resistance Changement of Compression Sensible Cement Speciment Under Different Stresses,* J. Wuhan University of Tech., 11(3), 1996, pp. 41-45.

11. Sun, M., Mao, Q. and Li, Z., *Size Effect and Loading Rate Dependence of the Pressure-Sensitivity of Carbon Fiber Reinforced Concrete (CFRC),* J. Wuhan University of Tech., Mater. Sci. Ed., pp. 58-61.

12. Shi, Z.-Q. and Chung, D.D.L., *Carbon Fiber Reinforced Concrete for Traffic Monitoring and Weighing in Motion,* Cem. Concr. Res., 29(3), 1999, pp. 435-439.

13. Hu, A., Fang, Y., Young, J.F. and Oh, Y.-J., *Humidity Dependence of Apparent Dielectric Constant for DSP Cement Materials at High Frequencies,* J. Amer. Ceramic Soc., 82(7), 1999, pp. 1741-1747.

14. Gu, P. and Beaudoin, J.J., *Dielectric Behaviour of Hardened Cement Paste Systems,* J. Mater. Sci., 15(2), 1996, pp. 182-184.

15. Zoughi, R., Gray, S.D. and Nowak, P.S., *Microwave Nondestructive Estimation of Cement Paste Compressive Strength,* ACI Mater. J., 92(1), 1995, pp. 64-70.

16. Janoo, V., Korhonen, C. and Hovan, M., *Measurement of Water Content in Portland Cement Concrete,* J. Transportation Eng., 125(3), 1999, 245-249.

17. Keddam, M., Takenouti, H., Novoa, X.R., Andrade, C. and Alonso, C., *Impedance Measurement on Cement Paste,* Cem. Concr. Res., 27(8), (1997) 1191-1201.

18. Alonso, C., Andrade, C., Keddam, M., Novoa, X.R. and Takenouti, H., *Study of the Dielectric Characteristics of Cement Paste,* Mater. Sci. Forum, 289-292(pt 1), 1998, pp. 15-28.

19. Al-Qadi, I.L., Haddad, R.H. and Riad, S.M., *Detection of Chlorides in Concrete Using Low Radio Frequencies,* J. Mater. Civil Eng., 9(1), 1997, pp. 29-34.

20. van Beek, A. and Hilhorst, M.A., *Dielectric Measurements to Characterize the Microstructural Changes of Young Concrete,* Heron, 44(1), 1999, 3-17.

21. El Hafiane, Y., Smith, A., Abelard, P., Bonnet, J.P. and Blanchart, P., *Dielectric characterization at High Frequency (1 MHz – 1.8 GHz) of a Portland Cement at the Early Stages of Hydration,* Ceramics-Silikaty, 43(2), 1999, 48-51.

22. Ford, S.J., Hwang, J.-H., Shane, J.D., Olson, R.A., Moss, G.M., Jennings, H.M., and Mason, T.O., *Dielectric Amplification in Cement Pastes,* Adv. Cem. Based Mater., 5(2), 1997, 41-48.

23. Miura, N., Shinyashiki, N., Yagihara, S. and Shiotsubo, M., *Microwave Dielectric Study of Water Structure in the Hydration Process of Cement Paste,* J. Amer. Ceramic Soc., 81(1), 1998, 213-216.

24. Ding, X.Z., Zhang, X., Ong, C.K., Tan, B.T.G. and Yang, J., *Study of Dielectric and Electrical Properties of Mortar in Early Hydration Period at Microwave Frequencies,* J. Mater. Sci., 31(20), 1996, 5339-5345.

25. Zhang, X., Ding, X.Z., Ong, C.K., Tan, B.T.G. and Yang, J., *Dielectric and Electrical Properties of Ordinary Portland Cement and Slag Cement in the Early Hydration Period,* J. Mater. Sci., 31(5), 1996, 1345-1352.

26. Yoon, S.S., Kim, H.C. and Hill, R.M., *Dielectric Response of Hydrating Porous Cement Paste,* J. Physics D – Applied Physics, 29(3), 1996, 869-875.

27. Al-Qadi, I.L., Hazim, O.A., Su, W. and Riad, S.M., *Dielectric Properties of Portland Cement Concrete at Low Radio Frequencies,* J. Mater. Civil Eng., 7(3), 1995, 192-198.

28. Zhang, X., Ding, X.Z., Lim, T.H., Ong, C.K., Tan, B.T.G. and Yang, J., *Microwave Study of Hydration of Slag Cement Blends in Early Period,* Cem. Concr. Res., 25(5), 1995, 1086-1094.

29. Olson, R.A., Moss, G.M., Christensen, B.J., Shane, J.D., Coverdale, R.T., Garboczi, E.J., Jennings, H.M. and Mason, T.O., *Microstructure-Electrical Property Relationships in Cement-Based Materials,* Proc. 1994 MRS Fall Meeting, Microstructure of Cement-Based Systems/Bonding and Interfaces in Cementitious Materials, Materials Research Society, Warrendale, PA, 370, 1995, pp. 255-264.

30. Haddad, R.H. and Al-Qadi, I.L., *Measuring Dielectric Properties of Concrete Over Low RF,* Proc. 1996 4th Materials Engineering Conference, Materials for the New Millennium, ASCE, New York, NY, 2, 1996, 1139-1149.

31. Gu, P. and Beaudoin, J.J., *Dielectric Behaviour of Hardened Cementitious Materials,* Adv. Cem. Res., 9(33), 1997, pp. 1-8.

32. Wen, S. and Chung, D.D.L., *Effect of Admixtures on the Dielectric Constant of Cement Paste,* Cem. Concr. Res., 31(4), 2001, pp. 673-677.

33. Sun, M., Liu, Q., Li, Z. and Hu, Y., *A Study of Piezoelectric Properties of Carbon Fiber Reinforced Concrete and Plain Cement Paste During Dynamic Loading,* Cem. Concr. Res., 30(10), 2000, pp. 1593-1595.

34. Wen, S. and Chung, D.D.L., *Effect of Stress on the Electric Polarization in Cement,* Cem. Concr. Res., 31(2), 2001, pp. 291-295.

Table 1. Measured longitudinal piezoelectric coupling coefficient d, measured relative dielectric constant κ, calculated piezoelectric voltage coefficient g and calculated voltage change resulting from a stress change of 1 kPa for a specimen thickness of 1 cm in the direction of polarization.

	Material	d (m/V)*	κ†	g (10^{-3} m^2/C)†	Voltage change (mV)†
(i)	Cement paste (plain)	3.0×10^{-13}	33	1.1	11
(ii)	Cement paste with steel fibers and PVA	2.5×10^{-11}	2500	1.1	11
(iii)	Cement paste with carbon fibers	4.3×10^{-13}	55	0.89	8.9
(iv)	PZT	1.4×10^{-11}	1000	1.5	15

*Averaged over the first half of the first stress cycle
†At 10 kHz

Table 2. Pyroelectric coefficient p at 20-28°C and various frequencies. (i), (ii) and (iii) are as defined in Table 1.

Cement paste	p (10^{-9} C/m^2.K)		
	10 kHz	100 kHz	1 MHz
(i)	0.28	0.16	0.14
(ii)	61	39	19
(iii)	3.5	2.4	1.8

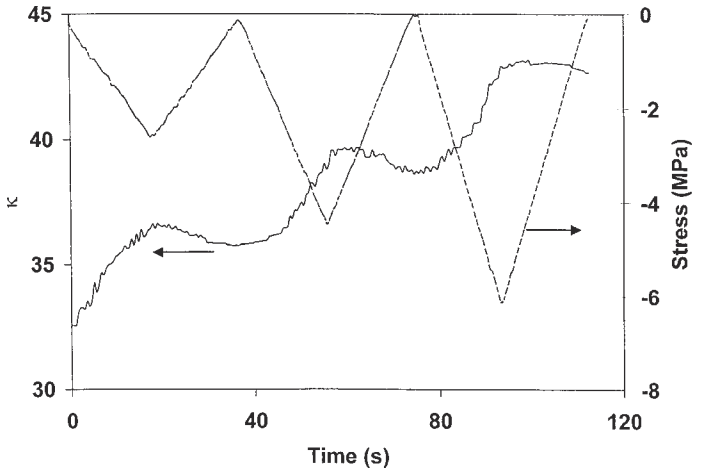

Figure 1—Variation of the relative dielectric constant κ (solid curve) with time, and of the stress (dashed curve) with time during repeated uniaxial compression of plain cement paste at increasing stress amplitudes.

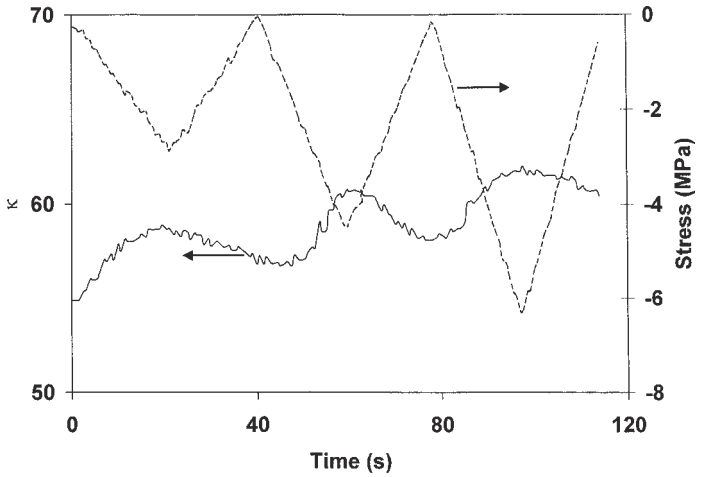

Figure 2—Variation of the relative dielectric constant κ (solid curve) with time, and of the stress (dashed curve) with time during repeated uniaxial compression of carbon fiber cement paste at increasing stress amplitudes.

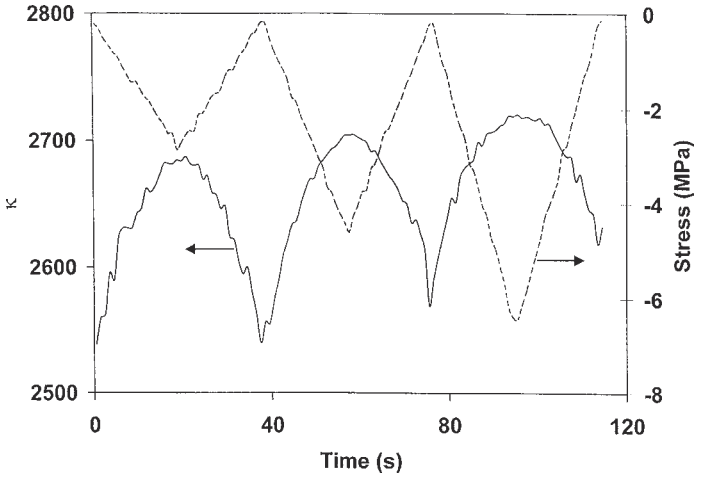

Figure 3—Variation of the relative dielectric constant κ (solid curve) with time, and of the stress (dashed curve) with time during repeated uniaxial compression of steel fiber cement paste at increasing stress amplitudes.

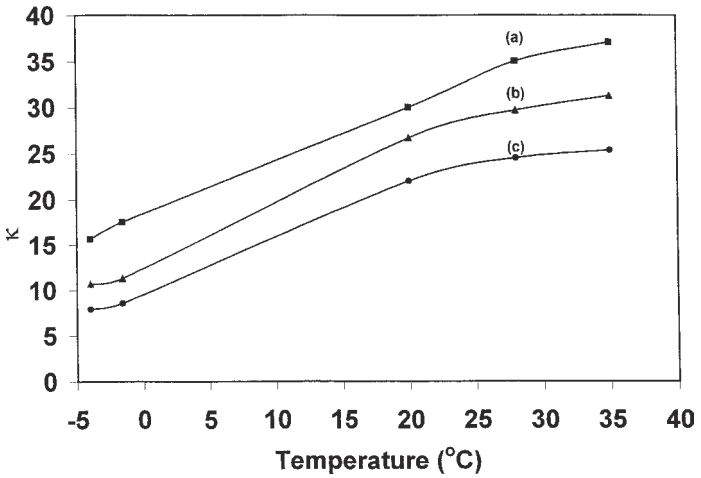

Figure 4—Variation of the relative dielectric constant κ of plain cement paste with temperature at (a) 10 kHz, (b) 100 kHz, and (c) 1 MHz.